On the Coupling between Magnetoelastic Waves and Nitrogen Vacancy Centers in Diamond

Adi Jung, ^{1,*} Samuel Margueron, ² Ausrine Bartasyte, ^{2,3,†} and Sayeef Salahuddin^{1,‡}

¹Department of Electrical Engineering, University of California, Berkeley

² FEMTO-ST Institute, University of Franche-Comté, **ENSMM**, 26 rue de l'Epitaphe, Besancon 25030, France

³ Institut Universitaire de France

(Dated: June 13, 2023)

We show that a strong coupling exists between Nitrogen Vacancy (NV) centers in diamond in proximity to magnetoelastic spin waves. Experimental measurements show the presence of both a linear and non-linear coupling. A model is proposed based on chiral coupling of the NV centers to the stray field that originates from the a propagating magnetoelastic wave in a thin magnet, and model predictions are validated by the experimental observations. Understanding of the coupling enables a direct measurement of the stray field polarization, which in turn provides a detailed picture of the resonantly coupled magnon-phonon interaction.

The phenomenon of magnetostriction was first reported and studied by Joule in 1847 [1]; over a century later, Charles Kittel would develop a theoretical framework for magnon-phonon interactions, predicting highly efficient power conversion between acoustic waves and magnetism [2]. Early experimental studies of high frequency magnetostrictive coupling relied on exciting magnetic resonance or high amplitude sound waves [3]; however, as nanofabrication technology developed, it became possible to efficiently excite GHz surface acoustic waves using high Q interdigitated transducers (IDTs) on piezoelectric substrates [4, 5]. As a result, in recent years, the number of studies of acoustically driven ferromagnetic resonance (ADFMR) [6–8] and other magnetoelastic effects has grown significantly [9, 10].

In this Letter, we show that a strong dipolar coupling can be achieved between ferromagnetic films undergoing acoustically-driven ferromagnetic resonance (ADFMR) and nitrogen vacancy (NV) color center in diamond [11] located nearby. We find that the coupling between the magnetic film and the NV centers is a combination of linear and nonlinear mechanisms, each with a distinct dependence on magnetic bias field. We propose a model that explains the observed phenomena. The coupling elucidates insight into the magnetoelastic dynamics and provides a pathway to study such dynamics with high spatial resolution, a capability that is not available in traditional spectroscopic techniques.

In Acoustically Driven Ferromagnetic Resonance, a voltage excites a Rayleigh wave in a piezoelectric material. When the Rayleigh wave passes through the magnetostrictive film sitting on top of the piezoelectric material, the acoustic wave induces an effective magnetoelastic field which converts acoustic energy into magnetic dynamics. With an appropriate balance of exter-

nally applied and internal anisotropy magnetic fields, the magnetization dynamics induce a resonance in the magnetostrictive film. The ADFMR device in this study consists of a piezoelectric substrate (128° Y-cut, Xpropagating LiNbO₃), on which interdigitated transducers were deposited and lift-off patterned (Al, 80 nm thick), exciting a Rayleigh-mode wave dominated by longitudinal strain. A magnetic film (Ni, 20 nm thick) was evaporated and lift-off patterned between the IDTs. Droplets of nanodiamonds containing NV centers (100nm diameter, 3 ppm NV concentration) were deposited on top of and adjacent to the Ni film, within the acoustic window of the IDTs; a diagram of the device is provided in Figure 1a. The LiNbO₃ / Ni bilayer was chosen as it is a model ADFMR system for which a large quantity of existing literature exists.

The NV center offers long room temperature spincoherence times [12] and a fluorescence readout mechanism implementable with relative ease in a benchtop optical system, and has been coupled to a range of magnetic systems in prior studies. In particular, it has been shown that NV centers can be used to directly image and quantify coherent spin-wave dynamics in a ferromagnetic film [13]. While the NV center is in principle capable of imaging spin-wave dynamics in acoustically-driven ferromagnetic systems as well, non-linear NV center coupling mechanisms exist in both resonant and acousticallydriven magnetic systems which are not present in traditional microwave drive [14, 15]. In this study, an IDT center frequency of 2.6 GHz was chosen to ensure that the 2.87 GHz NV center resonance would overlap with the drive frequency under Zeeman shift due to ADFMR bias fields in the Ni film.

To characterize the ADFMR-NV coupling, the device was mounted in a home-built 532 nm laser fluorescence microscope. First, ADFMR power absorption was characterized by driving the IDTs using a vector network analyzer (VNA) under a magnetic bias field sweep. The electrical S-parameters were time-gated to exclude elec-

^{*} adijung@berkeley.edu

 $^{^{\}dagger}$ ausrine.bartasyte@femto-st.fr

[‡] sayeef@berkeley.edu

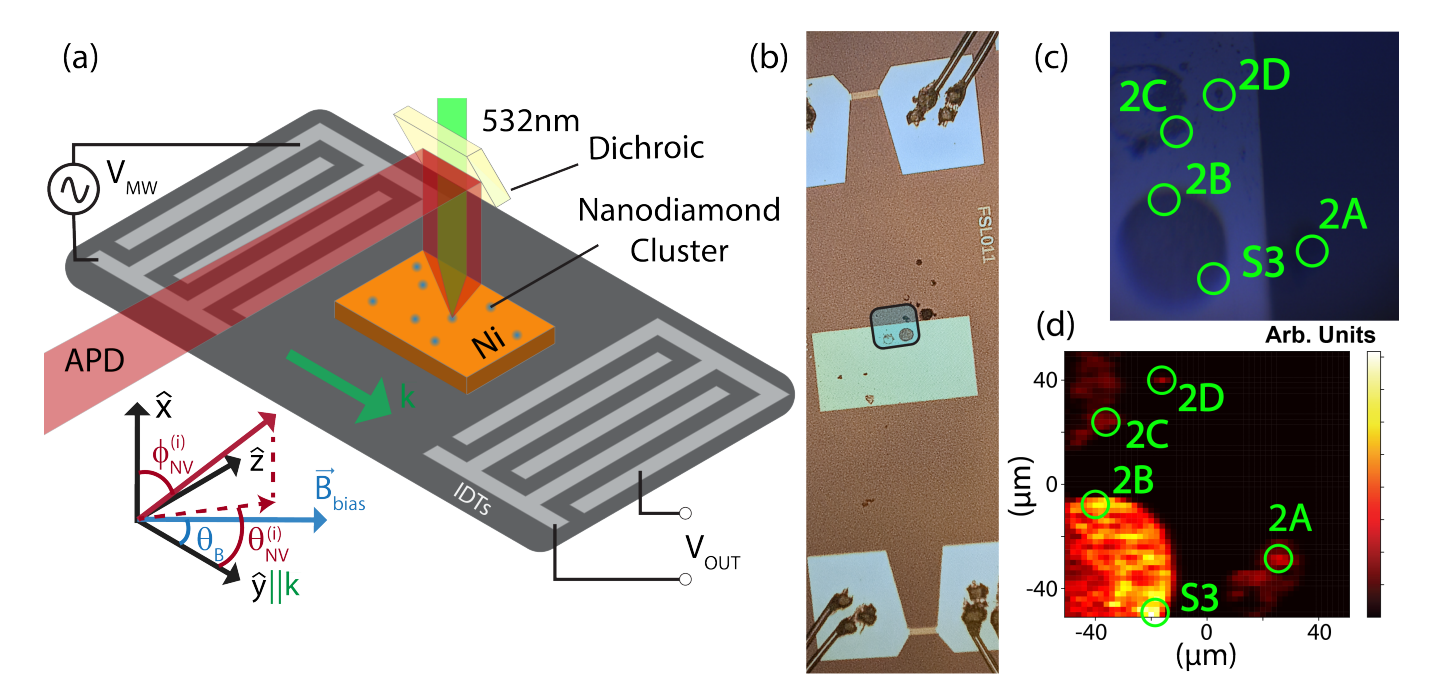


FIG. 1. Structure of the ADFMR Device. (a) Diagram of the overall experimental structure. Pulsed 532 nm light excites NV fluorescence, which is sensed by an APD. NV resonance is driven by magnetoelastic dynamics excited by the IDTs. (b) Optical image of the ADFMR device. Acoustic wave propagates from top to bottom; blue inset identifies the area characterized in (c-d). (c) Zoomed optical image of the NV clusters measured. Green circles identify locations where data was collected, and the corresponding figure in which the results are plotted. (d) Measured NV fluorescence intensity as a function of position. ODMR collection locations were chosen to be local fluorescence maxima.

tromagnetic coupling and triple-transit signals following standard ADFMR procedure [16]. Next, continuous wave NV ODMR was characterized under varying magnetic field bias in amplitude and direction. The transmitter IDT was driven by pulsed microwaves at +15 dBm, while pulsed 532 nm laser light excited the nanodiamond cluster of interest. The resulting NV fluorescence was isolated by a dichroic mirror and optical long-pass filter and measured using an avalanche photodiode (APD) and multi-demodulator lock-in amplifier.

To mitigate mechanical drift, data was collected at local maxima of NV fluorescence, and device position was periodically corrected to maximize NV fluorescence during the ~ 10 hour measurement, ensuring data was collected at the same location throughout. ODMR spectra were normalized to fluorescence intensity, and results are plotted in Figure 2. ODMR spectra were measured at multiple locations on the device, labeled in Figure 1cd. A control measurement was first taken at the NV center cluster off the Ni pad at location 2A. No synchronization of the lock-in amplifier with the microwave pulse frequency could be observed, indicating no dependence of fluorescence on acoustic drive and guaranteeing that the coupling mechanism is mediated by magnetic dynamics. Of the four locations where ODMR was measured, locations 2C and 2D corresponded to points near the center of the acoustic wave path where the acoustic amplitude was highest, and displayed nonlinear coupling. Locations 2B

and S3 were offset from the acoustic center, resulting in a lower acoustic amplitude, and displayed a linear coupling. Complete details of the experimental procedure are provided in the supplementary material.

The ODMR profile was also modeled within a proportionality factor through an analytical approach derivable from the NV center Hamiltonian and Maxwell's equations, following a combination of two experimentally validated models from literature [17][18]. The ODMR measured at location 2B is compared to the analytical model in Figure 3. Misalignment of the mounted device by 3.5° relative to the electromagnet poles leads to a corresponding rotation of the fluorescence spectrum. ODMR signal is maximized when the external applied field is offset by 90° from the acoustic propagation direction, matching the analytical model. The measured signal maximum occurs at a larger external field than modelled by approximately 23 G; this is attributed to stationary stray field from the Ni film, which is expected to reduce the effective magnetic bias field. Dipolar stray fields excited by the acoustic wave can be evaluated using a tensorial Green's function $\bar{G}(x-x')$ given by

$$\begin{pmatrix} \vec{H}_x(\vec{r}) \\ \vec{H}_y(\vec{r}) \\ \vec{H}_z(\vec{r}) \end{pmatrix} = e^{i\vec{k}_{\parallel} \cdot \vec{r}_{\parallel}} \int_{-t}^{0} dx' \bar{\bar{G}}(x - x') \begin{pmatrix} m_x(x') \\ m_y(x') \\ m_z(x') \end{pmatrix}$$
(1)

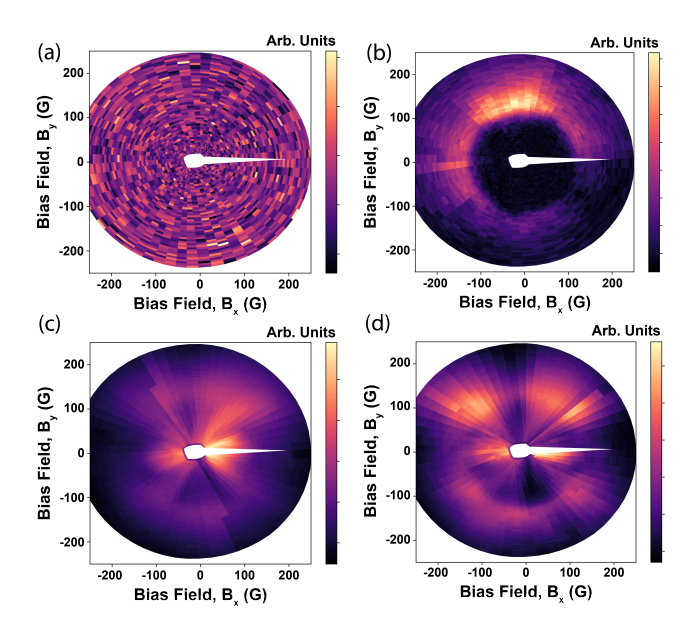


FIG. 2. ODMR signal versus magnetic bias field at nanodiamond clusters. Data near 0 field was not collected due to errors in the electromagnet power supplies at near-zero currents. (a) Control cluster off Ni pad. No fluorescence dependence on the MW drive was detected. (b) Cluster offset from acoustic path center, displaying Zeeman shift and angular dependence. See Figure 3 for analysis. (c) Cluster close to acoustic path center, see Figure 4 for analysis. Nonlinear coupling is observed, in line with prior NV-FMR studies. (d) Small cluster closest to the Ni pad edge; nonlinear coupling is expected to be strongest here. Qualitatively similar to (c).

$$\bar{\bar{G}}(x-x') = \frac{1}{2}e^{-ik_{\parallel}|x-x'|} \begin{pmatrix} k_{\parallel} & -ik_{y} & -ik_{z} \\ -ik_{y} & -\frac{k_{y}^{2}}{k_{\parallel}} & -\frac{k_{y}k_{z}}{k_{\parallel}} \\ -ik_{z} & -\frac{k_{y}k_{z}}{k_{\parallel}} & -\frac{k_{z}^{2}}{k_{\parallel}} \end{pmatrix}$$
(2)

The chiral response seen in Figure 3 emerges due to the fact that the acoustic wave induces a plane-wave magnetic excitation with matching wavevector and frequency and that the magnet precesses with a right circular polarization. Applying the magnetostatic approximation [19], the stray field above the magnetic film is also found to be circularly polarized, and proportional to

$$\begin{pmatrix} \vec{H}_x(\vec{r}) \\ \vec{H}_y(\vec{r}) \\ \vec{H}_z(\vec{r}) \end{pmatrix} \propto \begin{pmatrix} m_R(1+\sin\theta_B) + m_L(1-\sin\theta_B) \\ -i[m_R(1+\sin\theta_B) + m_L(1-\sin\theta_B)] \\ 0 \end{pmatrix}$$
(3)

where θ_B is the angle between bias field and acoustic wavevector. As a result, symmetry breaking in the angular ODMR profile is readily explained by chirality of dipolar stray fields[20]. Further details of the model are provided in the supplementary information.

The ODMR signal resulting from the stray field in (3) was evaluated by summing ODMR spectra of 1000 NV

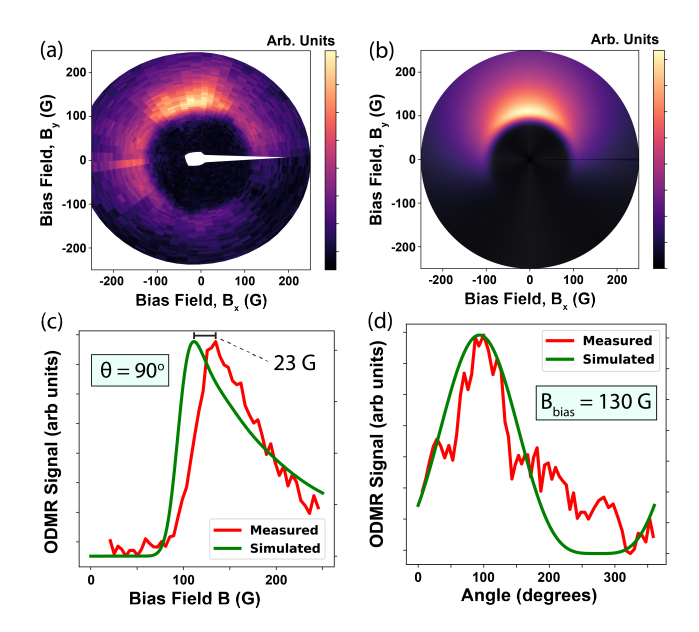


FIG. 3. Comparison of ODMR data in cluster 2B to model. (a) ODMR profile of Figure 2b. (b) Simulated ODMR profile for a circularly polarized spin-wave coupling to randomly oriented NV centers via dipolar fields. (c) Line-cut of (a-b) along $\theta_B = 90^{\circ}$, the measured signal maximum is found to be ~23 G higher than simulated. (d) Line-cut of (a-b) along $B_{bias} = 130$ G, showing a near identical angular signal dependence.

centers of randomly chosen orientation [18]. The ODMR signal was found to be proportional to κ , given by the expression:

$$\kappa^{(i)} = \langle \psi_f | \hat{H}_{MW}^{(i)} | \psi_i \rangle |^2 (\Delta \langle \hat{\rho} \rangle) (\Delta \langle \hat{S}_z^2 \rangle)$$

$$\Delta \langle \hat{\rho} \rangle = \langle \psi_f | \hat{\rho} | \psi_f \rangle - \langle \psi_i | \hat{\rho} | \psi_i \rangle$$

$$\Delta \langle \hat{S}_z^2 \rangle = \langle \psi_f | \hat{S}_z^2 | \psi_f \rangle - \langle \psi_i | \hat{S}_z^2 | \psi_i \rangle$$

$$\hat{\rho} = \hat{I} - \hat{S}_z^2$$

$$(4)$$

where $|\psi_i\rangle$ are eigenstates of the unperturbed Hamiltonian

$$\hat{H}_0 = D_{gs}(\hat{S}_{z'}^2 - \frac{1}{3}\hat{S}^2) + \gamma_e \hat{\vec{S}} \cdot \vec{B}_{bias}$$
 (5)

The perturbation Hamiltonian \hat{H}_{MW} induced by the spin wave stray field is evaluated numerically for each individual NV orientation. \hat{H}_{MW} is parameterized by the orientations of the NV axes and external bias field, and is given by the general equation:

$$\hat{H}_{MW}^{(i)} = h_{circ} * (f_x^{(i)}(\theta_B, \theta_{NV}^{(i)}, \phi_{NV}^{(i)}) \hat{S}_x + f_y^{(i)}(\theta_B, \theta_{NV}^{(i)}, \phi_{NV}^{(i)}) \hat{S}_y + f_z^{(i)}(\theta_B, \theta_{NV}^{(i)}, \phi_{NV}^{(i)}) \hat{S}_z)$$
(6)

The ODMR profile is modelled as a sum over NV orientations of Gaussian functions with amplitude κ and a linewidth of 54.2 MHz [18], a typical NV linewidth in nanodiamonds.

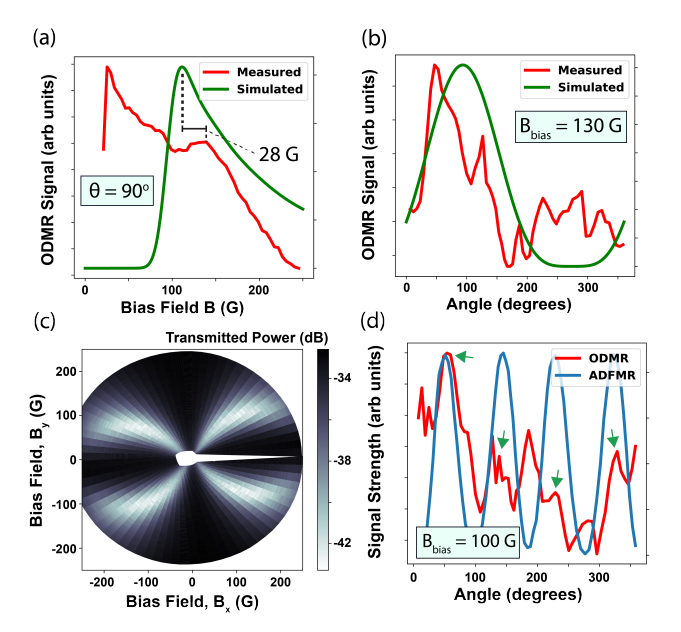


FIG. 4. Comparison of ODMR data in cluster 2C to model in Figure 3b. (a) Radial line-cut comparison at $\theta_B = 90^{\circ}$, large signals are observed near 0 field, attributed to incomplete saturation of the Ni film. (b) Angular line-cut comparison at $B_{bias} = 130$ G, highlighting the presence of a second, smaller lobe centered at 270° (c) Electrically characterized ADFMR absorption versus B_{bias} (d) Line-cut of measured ODMR and ADFMR signals in the nonlinear coupling region, assuming ADFMR absorption induces a field proportional to square root of absorbed power. Maximal ADFMR absorption angles coincide with ODMR maxima.

Turning to location 2C, discussed in Figure 4, we find that the ODMR profile at this position reflects both the linear coupling seen in location 2B and a nonlinear interaction coinciding with the acoustically-driven ferromagnetic resonance absorption. The typical theoretical framework of ADFMR models a Rayleigh-mode surface acoustic wave exciting a magnetostrictive thin film [21]. For a polycrystalline Ni film, the magnetoelastic free energy is given by [22]

$$G_{me} = b_1 \epsilon_{ij} m_i m_j \tag{7}$$

where ϵ represents the strain tensor, and m_i is the normalized magnetization in the \hat{i} direction. The acoustic wave modulates the magnetoelastic free energy, inducing an effective magnetoelastic field and converting acoustic energy into magnetic dynamics. For a longitudinal strain dominated acoustic wave, magnetoelastic power conversion is maximized in a 4-lobed angular pattern when the magnetization orientation is approximately at a $\pi/4$ angle to the acoustic propagation direction.

ADFMR absorption patterns and linewidth in Ni films have been well characterized in prior experiment, and

linewidth is known to be wider than electrically excited FMR linewidths in comparable Ni films [23]. As a result, we attribute the NV coupling with ADFMR absorption to a nonlinear resonant damping process where magnetic dynamics induce stray fields across a wide frequency band, some of which couple to the NV center clusters. Similar nonlinear behavior has been observed in other magnetic systems where NV centers have been coupled to uniform ferromagnetic resonance modes [15].

Interestingly, the largest NV-magnet coupling is observed to occur at low fields when external field is applied at angles of 0 and 180° to the wave propagation direction. This coupling occurs where nonlinear ADFMR lobe couplings are visible, but does not coincide with regions of high electrical absorption (see Supplementary Information). Notably, traditional ADFMR theory is predicated upon a complete saturation of the magnetization, but this approximation fails at low fields. It is expected that an unsaturated magnet going through resonance will excite a complex set of dynamics in the film. We hypothesize that the coupling observed at low fields is associated with incomplete saturation in the magnet and a complete picture in this context will need a revision of traditional ADFMR theory.

Our results demonstrate that multiple coupling mechanisms exists between magnetoelastic waves and NV centers and provide a methodology to distinguish between them. A linear, potentially coherent coupling between NV centers and magnetoelastic waves was experimentally shown, and validated by an analytical model based on chiral coupling of dipolar stray fields. Importantly, the chirality results in a circular polarization of the magneto elastic stray fields. In addition to the specificity it provides, it reduces the requirement for the drive power by a factor of $\sqrt{2}$ [24]. We have further characterized the nonlinear magnetic resonant coupling process known to occur in these systems, and shown that it occurs in conjunction with the linear coupling. Insight into the coupling mechanism allows one to use the NV centers to measure the polarization of the stray fields, as shown in this paper, which in turn carries the signature of the magnon-phonon interaction induced by ADFMR. In addition, NV centers have garnered great interest as extremely precise atomic sensors. Our work provides a pathway towards integrated atomic sensing, driven by purely voltage excitation, without needing any power hungry, external microwave excitation.

This work was supported by the NSF TANMS center within National Science Foundation Cooperative Agreement EEC-1160504. This work was also supported by the EIPHI Graduate School contract ANR 17 EURE 0002, the French RENATECH network and its FEMTO-ST technological facility.

The authors are grateful for fruitful discussions with Dr. Dominic Labanowski, Dr. Walid Redjem, and Dr. Satcher Hsieh.

- J. Joule, The London, Edinburgh and Dublin Philosophical Magazine and Journal of Science (Taylor & Francis, 1847).
- [2] C. Kittel, Interaction of Spin Waves and Ultrasonic Waves in Ferromagnetic Crystals, Physical Review 110, 836 (1958), publisher: American Physical Society.
- [3] G. C. Alexandrakis, R. a. B. Devine, and J. H. Abeles, High-frequency sound as a probe of exchange energy in nickel, Journal of Applied Physics 53, 2095 (1982), publisher: American Institute of Physics.
- [4] A. Mamishev, K. Sundara-Rajan, F. Yang, Y. Du, and M. Zahn, Interdigital sensors and transducers, Proceedings of the IEEE 92, 808 (2004), conference Name: Proceedings of the IEEE.
- [5] S. Gong and G. Piazza, Design and Analysis of Lithium-Niobate-Based High Electromechanical Coupling RF-MEMS Resonators for Wideband Filtering, IEEE Transactions on Microwave Theory and Techniques 61, 403 (2013), conference Name: IEEE Transactions on Microwave Theory and Techniques.
- [6] M. Küß, M. Heigl, L. Flacke, A. Hörner, M. Weiler, M. Albrecht, and A. Wixforth, Nonreciprocal Dzyaloshinskii-Moriya Magnetoacoustic Waves, Physical Review Letters 125, 217203 (2020), publisher: American Physical Society.
- [7] S. Alekseev, N. Polzikova, I. Kotelyanskii, and Y. Fetisov, Tunable HBAR based on magnetoelectric YIG/ZnO structure, in 2012 IEEE International Ultrasonics Symposium (2012) pp. 2481–2484, iSSN: 1051-0117.
- [8] S. Tiwari, J. D. Schneider, S. Wintz, S. S. P. K. Arekapudi, K. Lenz, A. Chavez, J. Lindner, O. Hellwig, G. P. Carman, and R. N. Candler, Coupling of Lamb Waves and Spin Waves in Multiferroic Heterostructures, Journal of Microelectromechanical Systems 29, 1121 (2020), conference Name: Journal of Microelectromechanical Systems.
- [9] Y. Kurimune, M. Matsuo, and Y. Nozaki, Observation of Gyromagnetic Spin Wave Resonance in NiFe Films, Physical Review Letters 124, 217205 (2020), publisher: American Physical Society.
- [10] P. G. Saiz, R. Fernández de Luis, A. Lasheras, M. I. Arriortua, and A. C. Lopes, Magnetoelastic Resonance Sensors: Principles, Applications, and Perspectives, ACS Sensors 7, 1248 (2022), publisher: American Chemical Society.
- [11] M. W. Doherty, N. B. Manson, P. Delaney, F. Jelezko, J. Wrachtrup, and L. C. L. Hollenberg, The nitrogenvacancy colour centre in diamond, Physics Reports 528, 1 (2013), arXiv:1302.3288 [cond-mat].
- [12] B. D. Wood, G. A. Stimpson, J. E. March, Y. N. D. Lekhai, C. J. Stephen, B. L. Green, A. C. Frangeskou, L. Ginés, S. Mandal, O. A. Williams, and G. W. Morley, Long spin coherence times of nitrogen vacancy centers in milled nanodiamonds, Physical Review B 105, 205401

- (2022), publisher: American Physical Society.
- [13] I. Bertelli, J. J. Carmiggelt, T. Yu, B. G. Simon, C. C. Pothoven, G. E. W. Bauer, Y. M. Blanter, J. Aarts, and T. van der Sar, Magnetic resonance imaging of spin-wave transport and interference in a magnetic insulator, Science Advances 6, eabd3556 (2020), publisher: American Association for the Advancement of Science.
- [14] D. Labanowski, V. P. Bhallamudi, Q. Guo, C. M. Purser, B. A. McCullian, P. C. Hammel, and S. Salahuddin, Voltage-driven, local, and efficient excitation of nitrogen-vacancy centers in diamond, Science Advances 4, eaat6574 (2018), publisher: American Association for the Advancement of Science.
- [15] C. S. Wolfe, V. P. Bhallamudi, H. L. Wang, C. H. Du, S. Manuilov, R. M. Teeling-Smith, A. J. Berger, R. Adur, F. Y. Yang, and P. C. Hammel, Off-resonant manipulation of spins in diamond via precessing magnetization of a proximal ferromagnet, Physical Review B 89, 180406 (2014), publisher: American Physical Society.
- [16] A. Jung, D. Macri, S. Margueron, A. Bartasyte, and S. Salahuddin, Double-peaked resonance in harmonicfree acoustically driven ferromagnetic resonance, Applied Physics Letters 119, 142403 (2021), publisher: American Institute of Physics.
- [17] T. Yu and G. E. W. Bauer, Chiral Coupling to Magnetodipolar Radiation (2020), arXiv:2001.06821 [condmat].
- [18] K. Jeong, A. J. Parker, R. H. Page, A. Pines, C. C. Vassiliou, and J. P. King, Understanding the Magnetic Resonance Spectrum of Nitrogen Vacancy Centers in an Ensemble of Randomly Oriented Nanodiamonds, The Journal of Physical Chemistry C 121, 21057 (2017), publisher: American Chemical Society.
- [19] J. D. Jackson, Classical Electrodynamics, 3rd ed. (Wiley, 1999).
- [20] T. Yu, C. Liu, H. Yu, Y. M. Blanter, and G. E. W. Bauer, Chiral excitation of spin waves in ferromagnetic films by magnetic nanowire gratings, Physical Review B 99, 134424 (2019), publisher: American Physical Society.
- [21] L. Dreher, M. Weiler, M. Pernpeintner, H. Huebl, R. Gross, M. S. Brandt, and S. T. B. Goennenwein, Surface acoustic wave driven ferromagnetic resonance in nickel thin films: Theory and experiment, Physical Review B 86, 134415 (2012), publisher: American Physical Society.
- [22] S. Chikazumi, Physics of Ferromagnetism (Clarendon Press, 1997).
- [23] D. Labanowski, A. Jung, and S. Salahuddin, Power absorption in acoustically driven ferromagnetic resonance, Applied Physics Letters 108, 022905 (2016), publisher: American Institute of Physics.
- [24] V. Yaroshenko, V. Soshenko, V. Vorobyov, S. Bolshedvorskii, E. Nenasheva, I. Kotel'nikov, A. Akimov, and P. Kapitanova, Circularly polarized microwave antenna for nitrogen vacancy centers in diamond, Review of Scientific Instruments 91, 035003 (2020), publisher: American Institute of Physics.